

Contents lists available at [ScienceDirect](http://www.sciencedirect.com)

Biochimica et Biophysica Acta

journal homepage: www.elsevier.com/locate/bbadis

scaRNAs regulate splicing and vertebrate heart development



Prakash Patil ^{a,1}, Nataliya Kibiryeveva ^{b,1}, Tamayo Uechi ^a, Jennifer Marshall ^b, James E. O'Brien Jr. ^b, Michael Artman ^c, Naoya Kenmochi ^{a,*}, Douglas C. Bittel ^{b,*}

^a Frontier Science Research Center, University of Miyazaki, Miyazaki, Japan

^b Ward Family Heart Center, Children's Mercy Hospital, University of Missouri–Kansas City School of Medicine, Kansas City, MO, USA

^c Department of Pediatrics, Children's Mercy Hospital, University of Missouri–Kansas City School of Medicine, Kansas City, MO, USA

ARTICLE INFO

Article history:

Received 27 January 2015

Received in revised form 30 March 2015

Accepted 14 April 2015

Available online 23 April 2015

Keywords:

Congenital heart defect

Tetralogy of Fallot

Splicing

Spliceosome

scaRNA

Zebrafish

ABSTRACT

Alternative splicing (AS) plays an important role in regulating mammalian heart development, but a link between misregulated splicing and congenital heart defects (CHDs) has not been shown. We reported that more than 50% of genes associated with heart development were alternatively spliced in the right ventricle (RV) of infants with tetralogy of Fallot (TOF). Moreover, there was a significant decrease in the level of 12 small cajal body-specific RNAs (scaRNAs) that direct the biochemical modification of specific nucleotides in spliceosomal RNAs. We sought to determine if scaRNA levels influence patterns of AS and heart development. We used primary cells derived from the RV of infants with TOF to show a direct link between scaRNA levels and splice isoforms of several genes that regulate heart development (e.g., *GATA4*, *NOTCH2*, *DAAM1*, *DICER1*, *MBNL1* and *MBNL2*). In addition, we used antisense morpholinos to knock down the expression of two scaRNAs (*scaRNA1* and *snord94*) in zebrafish and saw a corresponding disruption of heart development with an accompanying alteration in splice isoforms of cardiac regulatory genes. Based on these combined results, we hypothesize that scaRNA modification of spliceosomal RNAs assists in fine tuning the spliceosome for dynamic selection of mRNA splice isoforms. Our results are consistent with disruption of splicing patterns during early embryonic development leading to insufficient communication between the first and second heart fields, resulting in conotruncal misalignment and TOF. Our findings represent a new paradigm for determining the mechanisms underlying congenital cardiac malformations.

© 2015 The Authors. Published by Elsevier B.V. This is an open access article under the CC BY-NC-ND license (<http://creativecommons.org/licenses/by-nc-nd/4.0/>).

1. Introduction

Congenital heart disease (CHD) accounts for 25% of all birth defects and is a leading cause of death in children <1 year of age [1]. Nearly 80% of all CHD cases are idiopathic and multiple lines of evidence indicate a genetic contribution to CHD, but only relatively limited progress has been made in identifying the genetic basis of CHD [2,3]. Conotruncal defects, such as tetralogy of Fallot (TOF), result from disruption in the flow of tissue-specific information between the first and second heart fields at approximately 20 days of gestation. In the developing embryo,

precise spatial and temporal signaling is required between the first heart field from which the left ventricle is derived and the second heart field (SHF) from which the right ventricle (RV) and conotruncal outflow tract are derived [4–10]. Abnormal rotation of the SHF causes conotruncal malformations such as TOF. Development of the conotruncal outflow tract is mediated by multiple transcription factors (e.g., *NKX2.5*, *GATA4*) and gene networks, including the Wnt and NOTCH pathways. Although studies of the developing vertebrate heart have provided a framework of regulatory control, they have failed to define the underlying causes of the majority of CHDs.

The importance of noncoding RNA (ncRNA) for heart development has recently been shown to depend on the correct spatiotemporal expression of particular microRNAs [11]. In addition, there are clear spatial and temporal transcript splicing transitions that are conserved in the vertebrate heart during fetal and postnatal development [12,13]. Some exons are constitutive and are present in every mature message; however, there are many alternatively spliced genes/exons which are variably retained or excluded from a mature transcript that dramatically increase the complexity of the transcriptome and thus the proteome. Alternative splicing (AS) is temporally and spatially controlled resulting in unique splice variants in different tissues and at different time points

Abbreviations: AS, alternative splicing; CHDs, congenital heart defects; RV, right ventricle; TOF, tetralogy of Fallot; scaRNAs, small cajal body-specific RNAs; CHD, congenital heart disease; SHF, second heart field; ncRNA, noncoding RNA; snRNAs, small nuclear RNAs; snoRNAs, small nucleolar RNAs; rRNAs, ribosomal RNAs; TA, truncus arteriosus; PA/IVS, pulmonary atresia with intact ventricular septum; LNA, locked nucleic acid; qRT-PCR, quantitative RT-PCR; KUMC-MF, University of Kansas Medical Center–Microarray Facility; IPA, Ingenuity Pathways Analysis; RMA, Robust Multichip Analysis; FDR, false discovery rate; MOs, morpholino antisense oligos; hpf, hours post fertilization; RPKM, reads per kilobase of exon per million mapped reads; SMN, survival of motor neuron; SMA, spinal muscular atrophy; RP, retinitis pigmentosa

* Corresponding authors.

¹ These two authors made equal contributions to the paper.

<http://dx.doi.org/10.1016/j.bbadis.2015.04.016>

0925-4439/© 2015 The Authors. Published by Elsevier B.V. This is an open access article under the CC BY-NC-ND license (<http://creativecommons.org/licenses/by-nc-nd/4.0/>).

in the same tissue. The transition from a fetal to postnatal pattern of a conserved set of alternatively spliced isoforms was shown to be critical for mouse heart development [14]. Clearly, mRNA splicing plays a significant role in mammalian cardiac development, but the potential contribution to human heart pathology remains unknown.

The spliceosome facilitates pre-mRNA processing of most primary transcripts in eukaryotic genomes. The primary spliceosome, called the U2 spliceosome, is a multimegadalton ribonucleoprotein complex composed of numerous proteins and five small nuclear RNAs (snRNAs or spliceosomal RNAs: U1; U2; U4; U5; and U6). The conformation and composition of the spliceosome are highly dynamic and highly conserved across eukaryotes [15]. Elaborate RNA–RNA–protein interactions align the reactive subgroups and repeatedly rearrange as each intron is identified, intron–exon boundaries are located, and catalysis proceeds to remove each intron in every pre-mRNA.

As snRNAs mature they are themselves biochemically modified in a process directed by other small noncoding RNAs, the scaRNAs (small cajal body-specific RNAs). The scaRNAs are a subset of the small nucleolar RNA (snoRNA) family, which is a large family of conserved ncRNAs that primarily guide biochemical modifications of specific nucleotides (e.g., methylation and pseudouridylation) of ribosomal RNAs (rRNAs) and snRNAs. Without the specific modifications controlled by the scaRNAs, the spliceosome fails to function properly [16]. While the biochemical targets of snoRNAs have been clearly elucidated over the last 20 years, there is a paucity of information regarding the developmental significance of this abundant class of ncRNA.

We previously detected 135 snoRNAs (including 12 scaRNAs) of more than 900 snoRNA probes on an ncRNA array which were statistically differentially expressed in the right ventricles of infants with TOF relative to controls [17]. Most of these snoRNAs (126, 93%) had decreased expression. Remarkably, 115 (91% of 126 with reduced expression) had similarly reduced expression in the fetal myocardium relative to the control tissue [17]. Two snRNAs, U2 and U6, also had reduced expression levels in TOF and fetal tissue relative to control tissue. The 12 scaRNAs that were moderately reduced in TOF myocardium targeted only the snRNAs, U2 and U6. Furthermore, we observed alternative splice isoforms of genes that were enriched in genetic pathways that are known to be critical for heart development. This suggests the possibility of the failure of adequate regulation of the scaRNA level early in gestation and a potential impact on spliceosomal function through alteration of U2 and U6.

Studies of snoRNA-directed modification of ncRNA in bacteria and lower eukaryotes have shown that nucleotide modifications are important for stabilization, maturation, turnover and localization of ncRNAs [18,19]. However, similar studies in vertebrates have not been described until our recent report of the developmental significance of snoRNAs in zebrafish [20]. Impaired rRNA modification, even at a single site, led to severe morphological defects and embryonic lethality in zebrafish which suggests that rRNA modifications play an essential role in vertebrate development. Our studies highlight the importance of posttranscriptional modifications and their role in ncRNA function in higher eukaryotes. However, there are currently no reported studies of the role that scaRNAs play in regulating vertebrate development. Here we report the first investigation of scaRNA regulation of spliceosomal function and vertebrate development.

2. Material and methods

2.1. Derivation of primary cells

Tissue samples were collected at the time of surgical correction of TOF, truncus arteriosus (TA), and pulmonary atresia with intact ventricular septum (PA/IVS). All infants were less than one year of age and cytogenetic testing verified that none of the subjects had 22q11.2 deletions. Informed consent was obtained from a parent or legal guardian after reviewing the consent document and having their questions

answered (IRB # 11120627). Detailed subject descriptions were previously published [17,21]. Primary cell cultures were derived from RV tissue of infants with TOF. The RV tissue was immediately immersed in DMEM (Invitrogen/Gibco, Grand Island, NY) plus 10% fetal calf serum (Sigma/Safco, St. Louis, MO) and 1% pen/strep (Gibco). The tissue was minced and most of the media was removed, leaving only enough to keep the tissue from drying out. After 24 h, additional media was added and cells were growing robustly after 3 to 4 days. Media was exchanged every 48 h. In addition, we obtained a primary neonatal cardiomyocyte cell culture derived from normally developing human neonatal cardiac tissue from Celprogen (San Pedro, CA Cat#36044-21). These cells were also grown in DMEM plus 10% fetal calf serum and 1% pen/strep.

2.2. Transfection of scaRNA plasmids into primary cells

The expression vectors pCGL-SCARNA4 (ACA26) and pCGL-SCARNA1 (ACA35) were a generous gift from Dr. Tamas Kiss, Universite Paul Sabatier [22]. The scaRNAs were cloned into an intron sequence between hemoglobin exons 3 and 4 so that they would be correctly processed *in vivo* and expression was driven with the CMV promoter. We replaced SCARNA1 with the corresponding sequences from the scaRNAs: SNORD94, SCARNA8, SNORD67, and SCARNA23. The scaRNAs were transfected into the primary cell lines derived from infants with TOF according to the manufacturer's protocol. Briefly, 2 µg of plasmid DNA was diluted in 200 µl of serum free media and added to 2 µl of the Poly Magnetofectant (a magnetic nanoparticle transfection reagent; Oz Bioscience, France), vortexed and incubated for 20 min at room temperature. The transfection mixture was added dropwise to 2×10^5 cells in 1.8 ml of media containing 10% serum in a single well of a 6 well plate. The culture plate was set on top of a plate magnet (Oz Biosciences) for 20 min, and returned to the incubator. After 72 h, the cells were trypsinized, pelleted and stored at -80°C until processed for RNA extraction.

2.3. scaRNA knockdown

We used antisense LNA oligos (locked nucleic acid oligos, Exiqon Life Sciences, Woburn MA) to suppress the scaRNAs in primary cardiomyocytes as has been done previously in immortalized cell cultures [23,24]. Briefly, the LNA oligo protocol is as follows, 50 µM LNA oligo in 100 µl serum free media is mixed with 12 µl HiPerfect transfection reagent (Qiagen, Valencia, CA) and incubated for 20 min at room temperature. The transfection mixture was added to 2×10^5 cells in 2.3 ml of media with 10% serum in a single well of a 6 well cell culture plate. After 48 h, the cells were pelleted and stored at -80°C until processing. Identifying LNA oligos for effective knockdown of the scaRNA was an empirical process. Two to four oligos were tested for each scaRNA to determine which were most effective at knocking down the target scaRNA.

2.4. RNA isolation and qRT-PCR (human tissue)

RNA was extracted from $\sim 2 \times 10^6$ cells using a mirVana miRNA isolation kit (Invitrogen/Ambion) according to the manufacturer's instructions. Briefly, an equal quantity of total RNA (1 µg) together with random and oligo dT primers was reverse transcribed using Superscript III (Invitrogen by Life Technologies, Carlsbad, CA) according to the manufacturer's directions. Quantitative RT-PCR (qRT-PCR) was performed using Power SYBR Green PCR Master Mix (Applied Biosystems, Foster City, CA) according to the manufacturer's directions as previously described [21]. The reaction was carried out in an ABI7000 system (Applied Biosystems, Foster City, CA) beginning with 10 min at 95°C . The intensity of the SYBR Green fluorescence was measured at the extension step of each cycle. At least three replicates were performed on each sample for each gene. The primers for each scaRNA, snRNA and gene are given in Table S1. A dissociation curve was generated for all

reactions, and reactions were run on agarose gels to verify the presence of a single band. Normalization of the qRT-PCR reactions used the $2(-\Delta\Delta C^T)$ method using RNU24 and GAPDH as the standardization genes for each sample to correct for minor experimental error. Normalized C^T values were averaged to produce the mean C^T value. Primers for the qRT-PCR validation of variably spliced exons in genes from the Wnt pathway in zebrafish morphants are provided in Table S2. The values from the normally spliced exons were normalized using a constitutive exon from within the same gene.

2.5. Microarray analysis of splice variants

The exon arrays were AffymetrixHuEx-1_0-st-v2. The raw data for the arrays have been deposited in the Gene Expression Omnibus (miRNA arrays accession No. GSE35490) as described previously [17]. All arrays were run at the University of Kansas Medical Center-Microarray Facility (KUMC-MF) according to the manufacturer's protocols. KUMC-MF is supported by the University of Kansas, School of Medicine, KUMC Biotechnology Support Facility, the Smith Intellectual and Developmental Disabilities Research Center (HD02528), and the Kansas IDeA Network of Biomedical Research Excellence (RR016475). All statistical analyses were performed using statistical software: Partek Genomics Suite software version 6.6 (Partek Inc), and Bioinformatic assessment was done using Ingenuity Pathways Analysis (IPA, Ingenuity Systems, Inc Redwood City, CA). Raw data (CEL files) were uploaded into Partek Genomics Suite for normalization and statistical analysis. Robust Multichip Analysis (RMA) was used for background correction, followed by quintile normalization with baseline transformation to the median of the control samples. Only probes with intensity values >20% of background value, in at least 1 of the conditions, were included for additional analysis. A Student t test with a Benjamini and Hochberg multiple test correction for false discovery rate (FDR) was used to determine significance. Probes were filtered using an FDR-adjusted p value ≤ 0.05 . IPA was used to assess networks, functions, and/or canonical pathways represented by the list of alternatively spliced genes. Fisher's exact test was used to identify the most significantly ($p \leq 0.05$) altered biological functions and/or disease categories within the dataset.

2.6. Zebrafish

Zebrafish (*Danio rerio*, wild-type AB line) were raised and maintained under standard laboratory conditions at the Division of Bioresources, Frontier Science Research Center, University of Miyazaki, Japan. We targeted orthologous scaRNAs in zebrafish for knockdown with antisense morpholinos designed to inhibit scaRNA processing as previously described [20]. A database search for the 12 scaRNAs that were reduced in TOF revealed that 7 have homologs in zebrafish, including scarna1, scarna8, scarna13, scarna14 and scarna2 that carry out U2 snRNA modifications, and snord94 and snord7 which carry out U6 snRNA modifications. These "shared scaRNA targets" ensure the comparability and relevance of the data obtained from the zebrafish experiments to human heart development. We chose to focus on two scaRNAs scarna1 that targets U2 and snord94 that targets U6 as these are representative scaRNAs that had an impact on snRNA function when targeted in the human primary cell cultures.

2.7. Morpholino oligonucleotide injections and morphological analysis

Morpholino antisense oligos (MOs) to inhibit precursor scaRNA processing were obtained from Gene Tools, LLC (Philomath, OR, USA). The scarna1 and snord94 MOs were designed at the 3' end of scaRNA within the fifth intron of *ppp1r8b* and second intron of *rrm2* gene, respectively (Fig. S1). As a control, morpholinos with five mispaired bases (misMOs) were used. The sequences of the MOs are given in Table S3. Based on our previous methods [25], the MOs were injected into the

blastomere of one-cell stage embryos using an IM-30 Electric Microinjector (Narishige, Japan) at the following concentrations: snord94 MO at 5 $\mu\text{g}/\mu\text{l}$; and scarna1 MO at 10 $\mu\text{g}/\mu\text{l}$. The control MOs were injected using the same volume. We examined the effects of scaRNA suppression on heart development in zebrafish embryos by microscopic observation. The morphology and physiological function of zebrafish heart in morphants were analyzed by live-video imaging.

2.8. Northern blot analysis

The total RNA was extracted using TRIzol Reagent (Invitrogen, USA) according to the manufacturer's instructions. For each sample, 10 μg of total RNA was separated on a 1.5% denaturing agarose gel and blotted according to our previous procedures [20]. Briefly, the blots were hybridized overnight at 42 °C in modified Church-Gilbert hybridization buffer (0.5 M NaHPO₄, 1 mM EDTA, 0.5% BSA and 7% SDS) containing 1000 cpm LNA probes labeled with [γ -32P] ATP by T4 polynucleotide kinase (Takara, Japan). The probe sequences are listed in Table S3.

2.9. Semi-quantitative RT-PCR

The total RNA was isolated from 24–25 h post fertilization (hpf) embryos using a TRIzol Reagent method (Invitrogen, USA). Semi-quantitative RT-PCR was performed with 0.5 μg of total RNA as a template in a 20 μl reaction using a One-step RT-PCR kit (Qiagen, Germany). The RT-PCR conditions are as described in the manufacturer's protocol, except for a change in annealing temperature, which depended on the T_m value of the primers. The primer sequences for the genes are given in Table S3.

2.10. RNA-Seq analysis

Messenger RNA was extracted from zebrafish embryos at 6 and 24 hpf from wildtype embryos and embryos injected with antisense or mismatch morpholinos. Sequencing was done using an Illumina® Genome Analyzer™. Single-end mRNA-Seq reads were mapped to the zebrafish genome (danRar7), allowing up to two mismatches, using the STAR aligner and the Partek® Flow™ interface (Partek Inc. St. Louis, MO). The output BAM files were imported directly into Partek Genomics Suite 6.6 (PGS, Partek Inc. St. Louis, MO) and analyzed using the RNA-Seq interface. To detect differentially spliced genes, mRNA quantification was performed using the reads per kilobase of exon per Million mapped reads (RPKM) model for normalization [26]. Reads were assigned to individual transcripts/exons of a gene based on the Expectation/Maximization (E/M) algorithm [27] using the ENSEMBL database. Never the less, annotation of the zebrafish genome is limited with respect to splicing variants, so extensive analysis of genome-wide splicing was inadequate. We therefore focused on members of Wnt pathway which is more extensively annotated and also critical for regulating heart development. We evaluated exon retention in those genes using PGS ANOVA with a significant p-value ≤ 0.05 .

3. Results

3.1. Reduced noncoding RNAs and altered splicing patterns in primary cells

Our analyses of splicing variants in TOF myocardium using exon microarrays revealed a substantial number of genes that had significant differences in the patterns of splicing isoform expression in the RV from infants with TOF relative to the control RV. Furthermore, the genes with significant changes in isoforms were significantly enriched in networks known to be critical for regulating heart development {(i.e., Wnt, NOTCH, Sonic Hedgehog, BMP pathways $p < 0.01$, Fig. 1), see [17] for explanation of how cardiac list was derived}. Importantly, ~50% of these alternative isoforms are present in similar ratios in normal fetal RV relative to the RV of normally developing infants. Fig. 2 shows

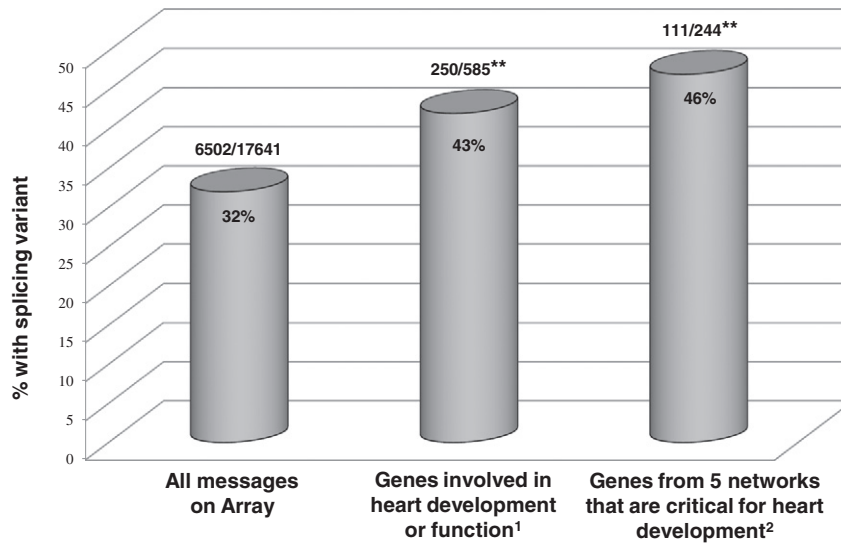


Fig. 1. Splicing variants detected in TOF RV vs. normal RV. Alternative splice variants in TOF RV are enriched in genes that are critical for heart development. Splicing analyzed using Partek Genomic Suite analytical software (including Bonferroni correction). 1st number is genes with alternative isoforms, 2nd number is total # of genes in the group. **Significantly different from “all messages” $p < 0.01$. 1. Cardiac Websites used to derive list: Cardiovascular Gene Ontology Annotation Initiative; CHD Wiki; HuGE Navigator (version 2.0). 2. Derived from Ingenuity Pathways Analysis.

representative examples of alternative splicing, *DICER* and *DAAM1*, which have a similar pattern of splicing in fetal and TOF tissues (blue and green lines) compared to the control tissue (red line).

We previously reported that 125 snoRNAs, including 12 scaRNAs, were downregulated in RV from 16 infants with TOF [17] (the scaRNAs are listed in Table 1 with their target nucleotides and known zebrafish homologs). In addition, U2 and U6 had significantly reduced expression in our 16 TOF RV samples compared to our 8 controls (analysis done by

microarray on 16 subjects; U2 was reduced 1.8 fold in TOF RV, $p = 0.04$, and U6 was reduced 3.2 fold in TOF RV $p < 0.0001$). We analyzed U2 and U6, and all 12 scaRNAs by qRT-PCR in the RV of an additional 24 samples from infants with TOF and all were consistently and significantly down-regulated compared to the 8 controls (data not shown). In these same 24 RV samples, we also used primers targeting the alternatively spliced exon (as shown in Fig. 2) to analyze by qRT-PCR the splicing of our six index genes (*GATA4*, *MBNL1*, *MBNL2*, *DICER*, *DAAM1* and *NOTCH2*)

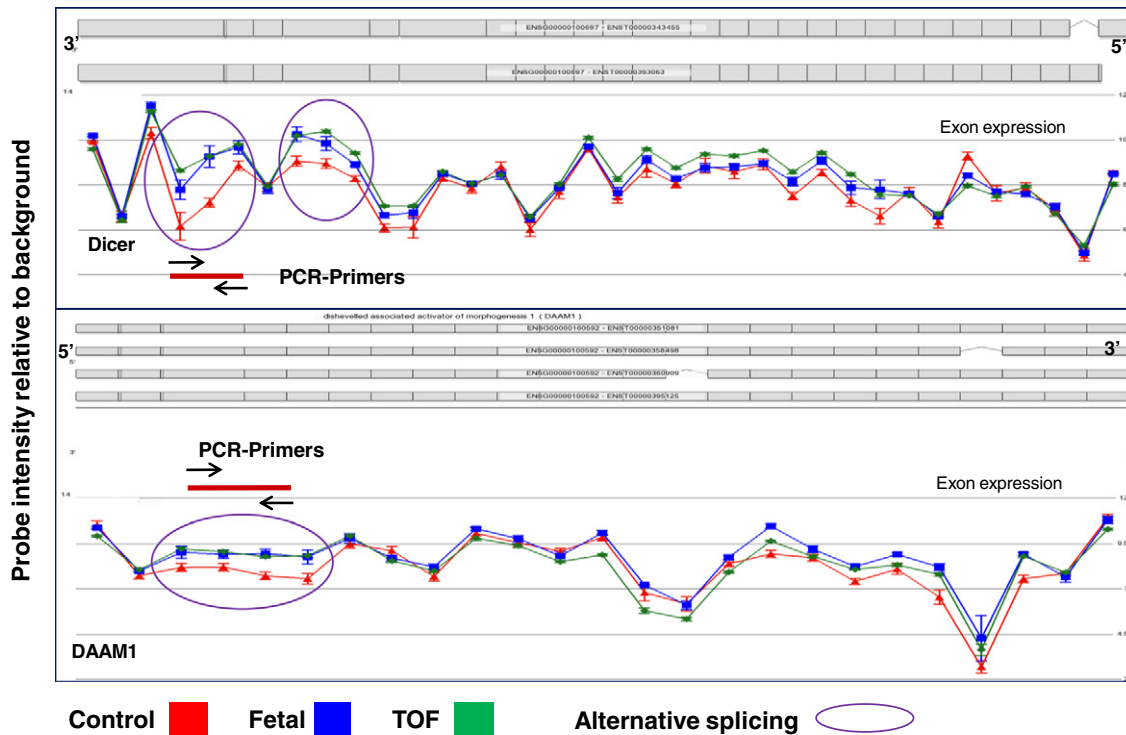


Fig. 2. Alternative splicing of some key genes resembles a fetal pattern. Red lines and arrows show position of primers used to amplify alternatively spliced region. The top section of each section shows known exons. The small boxes represent probe locations from the exon arrays. Bars around boxes are the standard deviation.

Table 1
scaRNAs with reduced expression in the right ventricle of infants with TOF.

scaRNA name	Zebrafish homolog	Target RNA and nucleotide(s) targeted	Chromosome	Start	Stop	Affy probeset ID	Host gene
Subcomponent of SCARNA2	No	U2 snRNA C61 and G11	chr1	109643155	109643234	HBII-382_s_st	
SCARNA9	Yes	U2 snRNA G19 and A30	chr11	93454680	93455032	mgU2-19-30	KIAA1731
SCARNA2	No	U2 snRNA G25 and C61	chr1	109642815	109643234	mgU2-25-61_st	
SCARNA8	Yes	U2 snRNA U34 and U44	chr9	19063654	19063784	U92_st	FAM29A
SCARNA4	No	U2 snRNA U41 and U39	chr1	155895749	155895877	ACA26_st	KIAA0907
SCARNA1	Yes	U2 snRNA U89	chr1	28160912	28161077	ACA35_st	PPP1R8
SNORD7	Yes	U6 snRNA A47	chr17	33900676	33900772	mgU6-47_st	
SNORD8	Yes	U6 snRNA A53	chr14	21865452	21865560	mgU6-53_st	CHD8
SNORD9	Yes	U6 snRNA A53	chr14	21860310	21860412	mgU6-53B_st	CHD8
SNORD67	No	U6 snRNA C60	chr11	46783939	46784049	HBII-166_st	CKAP5
SNORD94	Yes	U6 snRNA C62	chr2	86362993	86363129	U94_st	PTCD3
SCARNA23	No	U6 snRNA U40	chrX	24762558	24762687	ACA12_st	POLA1
SCARNA9L	No	U2 snRNA G19 and A30 (probable)	chrX	20154184	20154531	scaRNA-9L	EIF1AX

which are important for regulating cardiac development. These six genes had clear changes in splicing based on our microarray analysis of the right ventricle of all infants examined with TOF. Alternative splicing of the six index genes was highly consistent among the 24 additional samples analyzed by qRT-PCR, each sample having the pattern seen in the 16 samples analyzed by exon arrays.

Although it is beyond the scope of this report to extensively evaluate the proteomic impact of the alternative isoforms we describe, we used the UCSC and Ensemble Genome Browsers to examine the isoforms of our six index genes. Our six index genes all have alternative isoforms

that have all been previously reported and each isoform is known to be protein coding. The diagrams illustrating the data extracted from the browsers and the location of alternative spliced regions in our six index genes are shown in Supplemental Figs. 2–7.

3.2. Reduced scaRNAs, U2 and U6 expression, and alternative splicing are not a consequence of hypertrophy

Hypertrophy is known to induce gene expression patterns similar to those associated with fetal growth. To assess whether the altered

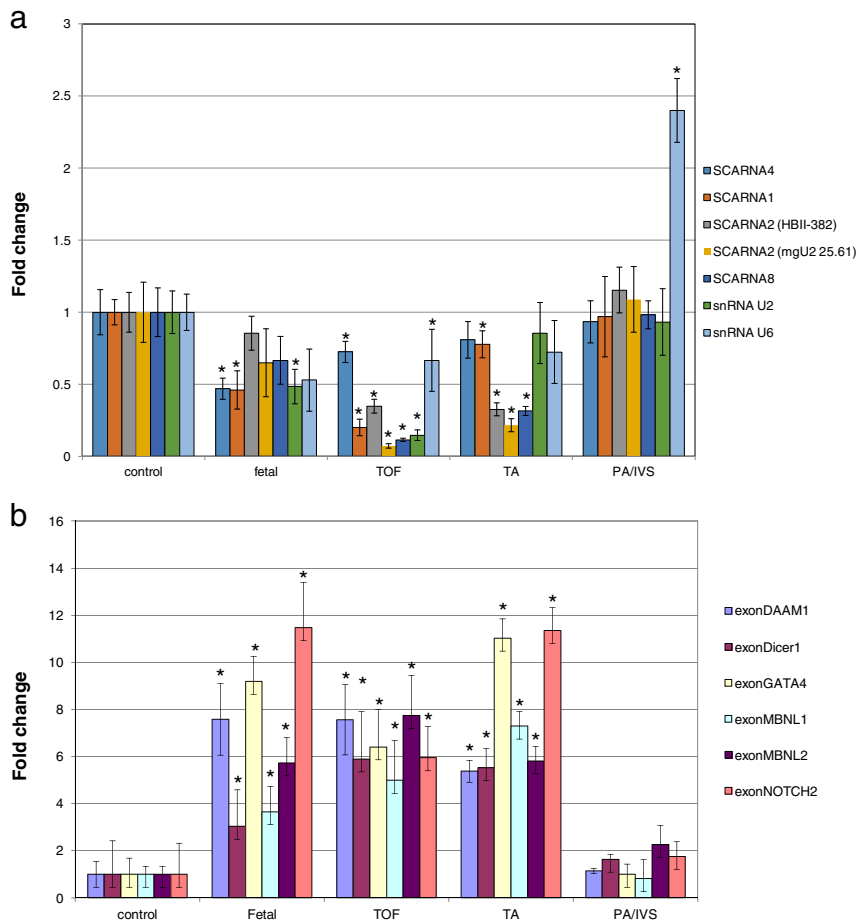


Fig. 3. scaRNA and splice variant levels in control and affected right ventricle. (A). scaRNA and splicesomal RNA levels in fetal TOF, TA and PA/IVS RV relative to control RV. Splicing variant assessed by qRT-PCR using primers specific to the variable exon. N = Control – 7, TOF – 31, Fetal – 6, TA – 3, PA/IVS – 3. *Significantly different from control, p < 0.05. (B). Variable exon splicing in RV tissue assessed by qRT-PCR using exon specific primers. Splice isoforms of index genes are similar in TOF and TA and fetal tissue, but PA/IVS does not differ from the control. N = Control – 7, TOF – 31, Fetal – 3, TA – 3, PA/IVS – 3. *Significantly different from control, p < 0.05.

expression and splicing observed in the RV of infants with TOF were a consequence of hypertrophy, we used qRT-PCR to assess the expression of U2 and U6, our 12 scaRNAs and the alternative splicing of our six index genes in RV samples from three infants with TA and three infants with PA/IVS. Both TA and PA/IVS are commonly associated with hypertrophy, as is TOF; however the three conditions may have different embryological origins. The qRT-PCR analysis of PA/IVS and TA samples indicated that U2 and U6 levels were not reduced in PA/IVS relative to the control tissue, but were significantly reduced in TA, similar to TOF relative to control RV. Furthermore, while none of the scaRNAs had changed expression in the PA/IVS-RV, they were all reduced in the TA-RV (Fig. 3A). Finally we assessed alternative splicing in our six index genes in PA/IVS and TA. The splice isoforms were unchanged relative to the controls in PA/IVS, while in TA-RV alternative splicing patterns were essentially the same as in TOF-RV (Fig. 3B). While this is not a transcriptome assessment, these data indicate that the changes we saw in snRNAs, scaRNAs and splicing in the TOF and TA samples were not simply a consequence of hypertrophy as they were not present in the PA/IVS samples which were also hypertrophic.

3.3. Alternative splicing occurs primarily in U2 type exons compared to U12 type exons

The spliceosomal RNAs, U2 and U6 are part of the U2 spliceosome, but there is a secondary spliceosome, termed U12, that is structurally and functionally analogous to the U2 spliceosome but does not use the U2 and U6 snRNAs [28]. The U12 spliceosome mediates the excision of a minor class of evolutionarily conserved introns that have non-canonical recognition sequences that are distinct from those recognized by the U2 spliceosome. The U12 spliceosome accounts for approximately 0.5% of exon/intron splicing. We used the U12 database (U12DB at <http://genome.imim.es/cgi-bin/u12db/u12db.cgi>) to identify genes that contain exons with U12 splicing recognition sequences. We used our exon array data (GEO # GSE35490) to compare the frequency of alternative splicing between U2 and U12-targeted exon/introns in the myocardium from normally developing infants and infants with TOF. Of the 229 genes in the five networks associated with heart development found on our exon arrays from our TOF-RV samples, 117 (51%) had significantly altered splicing patterns, of which >25% were in common with fetal tissues compared to RV from normally developing infants. We found 464 genes with U12 type exons on our array and 22(4.8%) of them had significant alternative splicing events in TOF myocardium. These two proportions (51% vs. 4.8%) are significantly different ($p < 0.0001$) indicating that splicing variation was significantly higher in U2 type exons compared to U12 type exons in myocardium from infants with TOF. In addition, the 464 genes with U12 intron/exon junctions had 1191 exons/introns targeted by the U12 spliceosome, of which 26 exons/introns were alternatively spliced (2.2%). The 229 genes from the five cardiac networks had 3429 exon/intron units of which 408 were alternatively spliced (12%).

3.4. Primary cells derived from TOF myocardium retain the same relative splicing and expression patterns as the tissue

We derived primary cell lines from right ventricular myocardium obtained from 10 infants with TOF (TOF primary cells, referred to after this as TOFpCs). We extracted RNA from the TOFpCs and examined expression patterns of scaRNAs, spliceosomal RNAs and mRNA splicing from the six index genes that were alternatively spliced in TOF RV tissue (Table 2). TOFpCs retained the same fetal type pattern of scaRNA and spliceosomal RNA expression relative to cells derived from normally developing neonatal cardiac primary cells. Splicing patterns also remained similar in the TOFpCs relative to the tissue they were derived from. Table 2 shows examples of qRT-PCR assessment of alternatively spliced isoforms (a measure of retained fetal exons) in the index genes from two independently derived TOFpCs compared to cells

Table 2

Fetal splice isoforms are overexpressed in TOF myocardium and in TOF primary cells (qRT-PCR, fold change in fetal exons).

Gene (exon of fetal isoform)	Normal myocardium	TOF myocardium	Normal primary cardiomyocyte cells	TOFpC31	TOFpC44
DICER	1	+2.8	1	+2.6	+4.6
DAAM1	1	+4.8	1	+3.0	+3.9
GATA4	1	+10.0	1	+8.8	+13.2
NOTCH2	1	+4.3	1	+6.0	+20.8
MBNL1	1	+6.7	1	+17.9	+26.5
MBNL2	1	+8.4	1	+9.5	+12.1

derived from normally developing heart tissue. In addition, the splicing and expression patterns were evaluated in the other eight independent cell lines and all were consistent.

3.5. Overexpression and knockdown of scaRNAs in primary cells cause changes in splicing

In order to investigate whether the alternative splicing we demonstrated in tissues and cells derived from patients with TOF was a consequence of changes in levels of scaRNAs, we used the expression plasmids pCGL-SCARNA4 and pCGL-SCARNA1 to induce expression of the respective scaRNAs in primary cells derived from infants with TOF. When either plasmid was transfected alone there was an increase in the scaRNA but no change in U2 level (the snRNA targeted by SCARNA4 and SCARNA1) nor any change in other spliceosomal RNAs, and no detectable change in splicing (data not shown). However, when we simultaneously transfected plasmids pCGL-SCARNA4 and pCGL-SCARNA1 into TOF primary myocytes, there was a modest (~1.8 fold) but significant upregulation in the amount of U2 (Fig. 4A). There was no change in the level of U6 or any other spliceosomal RNA tested. Importantly, there was a significant reduction in the level of the fetal type splice forms in the index genes (Fig. 4B). These experiments were repeated in primary cells derived from the RV of three different infants with TOF (three different genotypes). Fig. 4 compares transfected TOF cells to nontransfected TOF cells and normal cells. We transfected single plasmids in concentrations equal to the total plasmid concentration used in double transfections and saw a dose response in the amount of scaRNA in the single plasmid transfection but no change in splicing or target spliceosomal RNA level or cell viability (data not shown). Thus the affect seen by dual plasmid transfection appears to be the consequence of synergistic effect and not due to plasmid overload.

We knocked down single scaRNAs (SCARNA1 and SCARNA4) in cardiomyocytes from normally developing infants. The targeted scaRNAs were reduced but single knockdown experiments did not affect U2 levels or splice isoform levels (data not shown). This is not surprising as multiple scaRNAs probably need to be targeted to have a significant downstream impact, as we saw with upregulation of the scaRNAs. When we knocked down both SCARNA1 and SCARNA4 simultaneously, we saw a modest but significant decrease in the level of U2 (~65%, $p < 0.001$) with no change in U6 level (performed on two independent cell lines). In addition, after knocking down both scaRNAs we saw changes in splicing of some of our index genes, but the changes were not necessarily the same as the splicing patterns observed in the TOF tissue.

3.6. scaRNA levels and splicing patterns change during zebrafish development

There is little known about alternative splicing of mRNA during zebrafish development. Therefore, we downloaded RNA-Seq data from the Gene Expression Omnibus derived from developing zebrafish

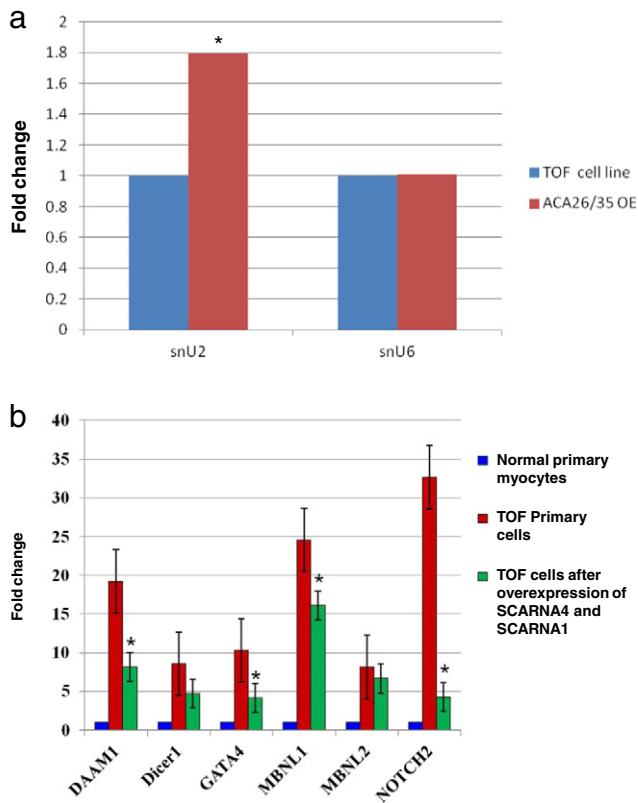


Fig. 4. A. U2 level increase after overexpression of scaRNAs. Data are fold change, averaged from three different primary myocyte cell lines. *Significant difference, $p < 0.01$, ** $p < 0.001$. The level of spliceosomal RNAs, U2 and U6, are significantly lower in primary cells from TOF compared to normal cardiomyocytes. U2 is significantly increased in primary cells from TOF after transfection with the both scaRNA expression plasmids containing ACA26 and ACA35 compared to normal cardiomyocytes, while U6 is unchanged. U2 and U6 levels were unchanged after transfection with single plasmids with total plasmid concentration equal to the combined plasmid concentration of double transfections. Data not shown. B. Fetal splice isoforms are reduced after overexpression of scaRNAs. Data are fold change, averaged from three different primary myocyte cell lines. *Significant difference between primary cells with over expressed scaRNAs vs TOF primary cells, $p < 0.05$. Expression plasmids pCGL-SCARNA4 and pCGLSCARNA1^{1,2} were a generous gift from Dr. Tamas Kiss, Universite Paul Sabatier, France.

embryos at 0.75 h, 6 h, 1 day, 2 days, 3 days and 5 days post fertilization (GEO#: [GSE30603](#)) and analyzed it for alternative splicing and changes in scaRNA expression during normal developmental progression in zebrafish. We reanalyzed the files to identify snoRNA and scaRNA sequences within the data. We identified 74 snoRNAs and scaRNAs within the zebrafish genome. Many snoRNAs varied significantly over the developmental time course (Fig. S2). We were particularly interested in scarna1 and snord94 since they influenced the spliceosomal RNA levels in our experiments using human primary cells. Their expression patterns varied dramatically as development progressed (Fig. S9A and B). Although, the current knowledge regarding splice variants within the zebrafish genome is only rudimentary, we found clear changes in ratios of splice isoforms of many of genes, including genes that are important for heart development (representative examples: *gata4*, Fig. S10 and *dicer*, Fig. S11).

3.7. Inhibition of scaRNA expression alters heart morphology and splicing in zebrafish

We inhibited the scaRNA expression in zebrafish using precursor-MO, which inhibits scaRNA precursor processing and thus reduces the level of the mature scaRNA [20]. The MOs were designed to target the precursor sequence of the scaRNAs (snord94 and scarna1) located within the introns of gene (Fig. S1). Loss of scaRNA expression was

confirmed by northern blot analysis of total RNA that was extracted from MO-injected embryos (MO, Fig. 5). Northern blot analysis showed a decrease in mature snord94 expression with the snord94 MO, but mature scarna1 expression is unaltered in these morphants. This demonstrates that the snord94 MO specifically inhibited snord94 scaRNA synthesis (Fig. 5A). Similarly, scarna1 synthesis is specifically suppressed in scarna1 MO injected embryos. In addition, semi-quantitative RT-PCR analysis revealed that scaRNA precursor inhibition using either snord94 or scarna1 MO did not affect the host gene splicing in morphants (Fig. 5B). In addition, RNA-Seq data also supported the loss of scarna1 and snord94 when targeted by antisense morpholinos as each was undetectable at 24 h when targeted (Figs. S12 and S13, respectively).

We performed the phenotypic analysis of scaRNA-deficient embryos at various stages of development. Loss of scaRNA expression resulted in growth impairment and specific developmental abnormalities, primarily involving heart malformations. At 25 hpf, both the scarna1 and snord94 MO-injected embryos showed little developmental delay with slightly changed eye and head size, and bent tail (Fig. 6A). However, there were no defects in the brain, notochord, otic vesicles and fins, except the deformed yolk sac and pericardial edema, were more conspicuous at 50 hpf compared to uninjected embryos (Fig. S8). There were obvious changes in the shape and size of the heart leading to its malformation, that was more significant in morphants by 72 hpf (Fig. 6B and Fig. S14 and Supplemental videos). The control mismatch MO-injected embryos developed normally with no discernable differences compared to uninjected embryos.

We analyzed splicing using RNA-Seq in zebrafish at 6 hpf and 24 hpf in wildtype, and after injection of antisense and missense morpholinos at the one cell stage. The annotation of the zebrafish genome is rudimentary for RNA-Seq assessment, especially with respect to splicing variation. We therefore, focused on the Wnt pathway for assessment of alternative splicing due to its being a key pathway for regulating heart development and because it is currently more fully annotated in the zebrafish genome. We saw clear evidence of alternative exon inclusion or exclusion after antisense morpholino injection for 13 of the 39 Wnt pathway genes that are identifiable in the zebrafish genome in the UCSC genome browser. We used qRT-PCR to validate the Wnt pathway members with altered exon retention, as well as, *gata4* and *mbnl1* (Fig. 7A–D and Fig. 8). The qRT-PCR values of variable exons were normalized to constitutive (nonvariable) exons from within the same gene. Table S2 lists the qRT-PCR primer sequences used for validation. We used qRT-PCR to examine these same 13 genes in the snord94 MO morphants (Fig. S15). Although the pattern of change was not exactly the same, 12 of the 13 Wnt genes had altered splicing patterns in the snord94 MO morphants as well.

4. Discussion

4.1. Hypertrophy is not the cause of altered expression or splice variants

Coordinated control of alternative splicing modifies the transcriptome and increases the complexity of the proteome during most developmental processes [29,30]. Studies of animal models have shown the importance of appropriate splicing for proper heart development [8,12,31,32]. Still, knowledge of the sequence of events leading to tissue specific alternative splicing is incomplete. We previously identified alterations in mRNA splice isoforms and in scaRNA expression patterns associated with tetralogy of Fallot [17]. In addition, these patterns resembled patterns we observed in fetal heart tissue. It has been shown that hypertrophy can reactivate genes that are expressed during fetal development. We analyzed scaRNA expression and splicing patterns of key index genes that regulate heart development in the RV of infants with PA/IVS and TA to determine if hypertrophy could be reactivating a fetal pattern of ncRNA expression and/or splicing. The embryological origin of TOF and TA may share some common features involving the

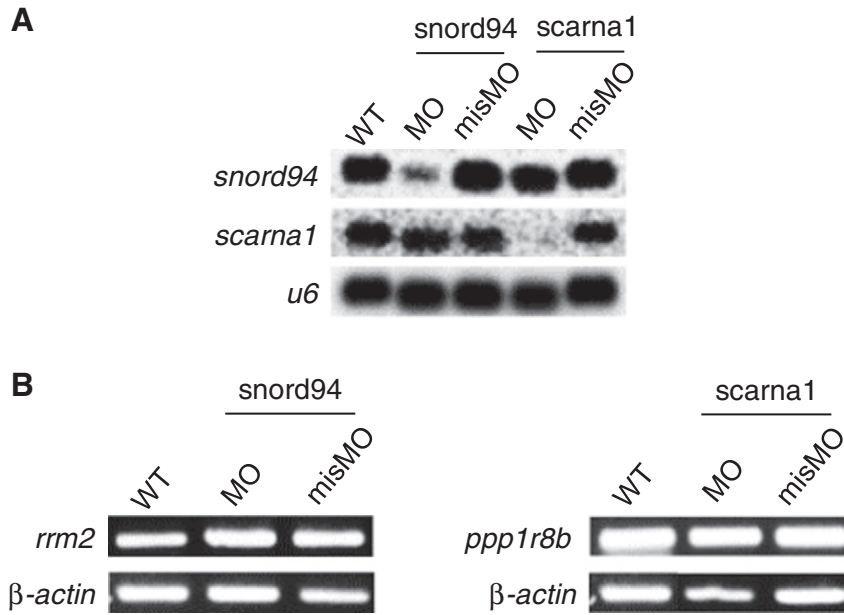


Fig. 5. Reduced expression of snord94 and scarna1 in MO-injected zebrafish. (A). Northern blot analysis of total RNA extracted from MO-injected embryos. B. Semi-quantitative PCR of host gene mRNA using either snord94MO or scarna1MO or mismatch morpholinos.

first and second heart field; however, PA/IVS is clinically distinct from TOF or TA and probably has a distinctly different etiology. Importantly hypertrophy is associated with all three developmental defects. In RV from infants with PA/IVS, we saw no change in scaRNA levels (only 10 snoRNAs had significant changes), nor any change in splicing compared to RV from normally developing infants. However, all 12 scaRNAs examined and the splicing patterns of our index genes in the RV from infants with TA were significantly altered compared to controls and were essentially the same as samples from infants with TOF as well as the

fetal pattern. This strongly suggests that the changes we saw in scaRNA expression and alternative splicing are not due to reactivation of fetal expression patterns as a consequence of hypertrophy.

4.2. Exons spliced by the U2 spliceosome are impacted by scaRNA expression changes

Furthermore, we assessed the specificity of the scaRNA dysregulation in our TOF samples by comparing splicing of exons/introns targeted by

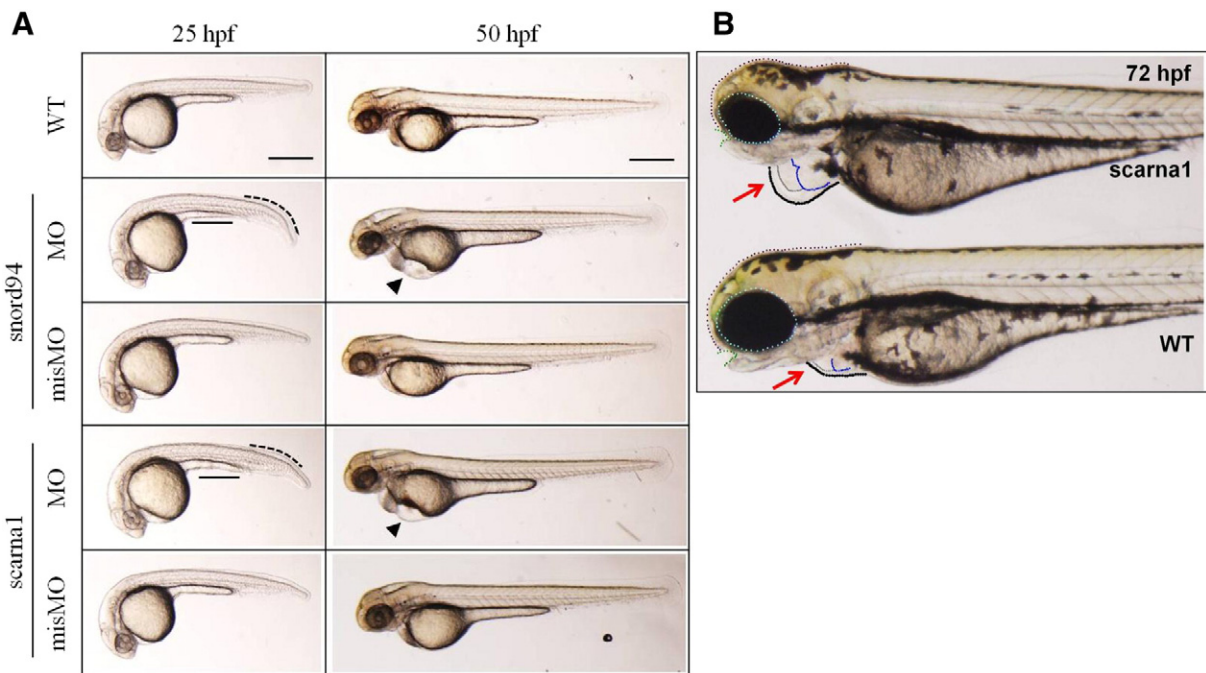


Fig. 6. Heart deformities in MO-injected zebrafish. (A) Lateral views of wild-type and MO-injected embryos at 25 and 50 hpf. Both the snord94 and scarna1 morphants display little developmental delay with bent tail (black dotted curved line) and improperly formed yolk extension (black solid line) at 25 hpf. The pericardial edema (black triangle) and deformed yolk sac were more evident at 50 hpf. (B) Enlarged images of the heart region in wild-type and MO-injected embryos at 72 hpf. The conspicuous pericardial edema (black dotted circle) was observed in snoRNA MO-injected embryos. Gray outline is the atrium, blue outline is the ventricle. Scale bars: 200 μ m.

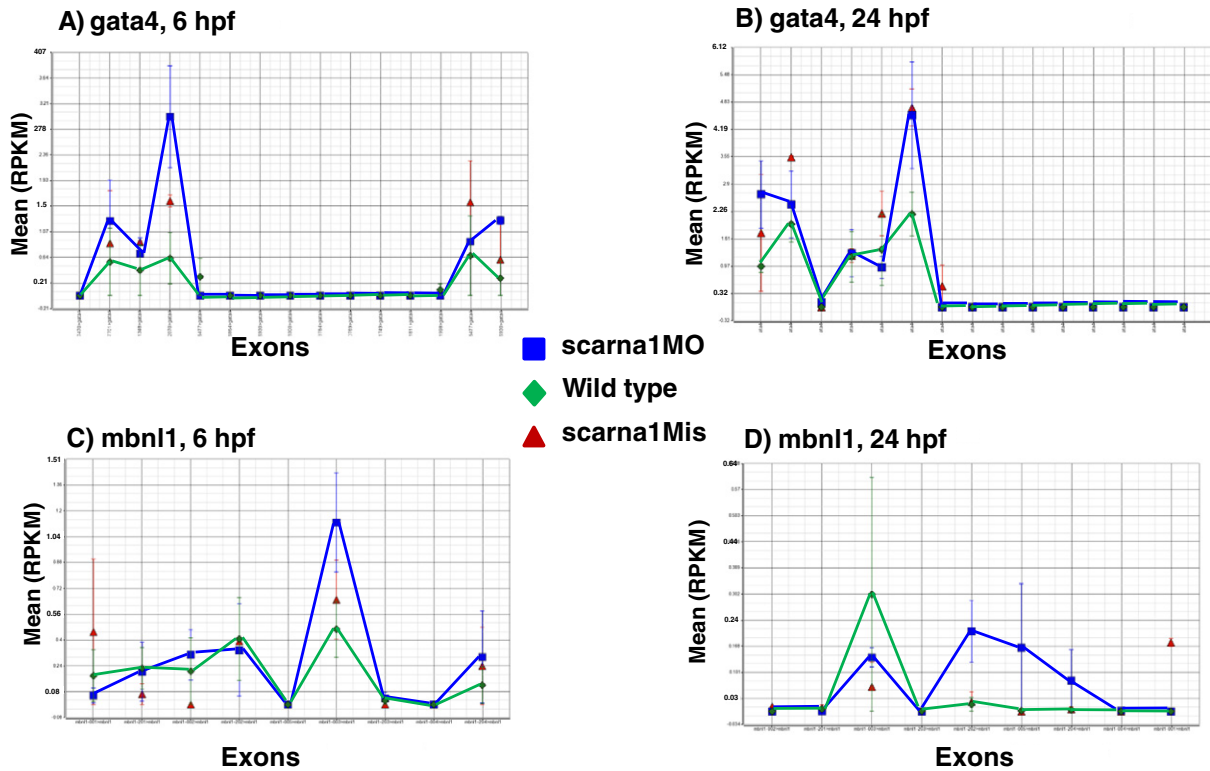


Fig. 7. Representative examples of splice isoform variation (exon retention) after treating zebrafish embryos with anti-scarna1 morpholino. Each point on the horizontal axis represents an exon and the value represents the mean RPKM (reads per kilobase per million) for that exon. Gata4 and Mbn1, 6 and 24 h post fertilization (hpf).

the U2 spliceosome compared to those targeted by the U12 spliceosome. A small percentage (4.8%) of U12 targeted splice sites were altered in the RV of infants with TOF when compared to the RV of normally developing infants. However, this was significantly less than the general group of genes processed by the U2 spliceosome. An even greater difference was seen in the splicing pattern of genes known to participate in regulating heart development, in which 51% had alternative forms present in the infants with TOF (significance $p < 0.0001$ compared to 4.8% of genes processed by U12). There may have been other factors affecting splicing, but these data suggest that the reduced expression of these scaRNAs did not

simply cause random changes in exon retention/exclusion and supports the possibility of targeted effects on the spliceosome resulting in specific alternative splicing.

4.3. Altered expression of scaRNAs causes changes in splicing

We used primary cells derived from the RV of infants with TOF to study the effects of altered expression levels of specific scaRNAs on the spliceosomal RNA they targeted and on splicing. Transfection of a single scaRNA expression vector resulted in a significant increase in

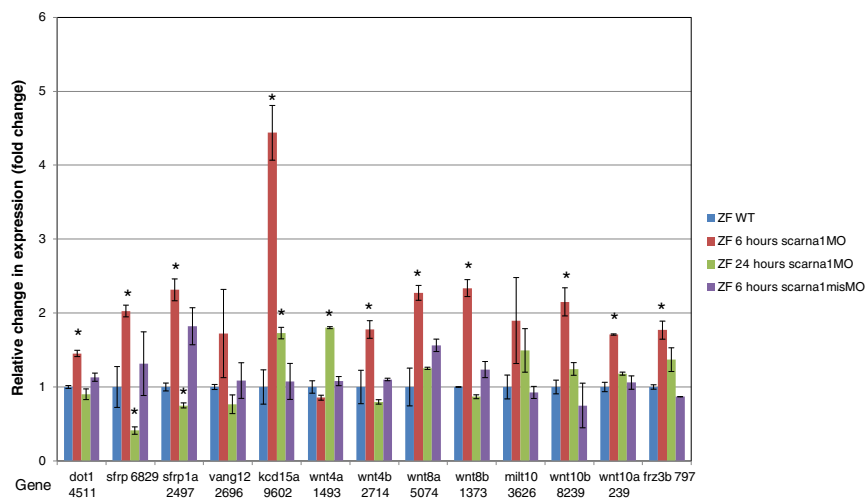


Fig. 8. Splice isoform changes after targeting scarna1. Treating zebrafish embryos with anti-scarna1 morpholino causes changes in exon retention of cardiac regulatory genes. 13 of 39 members of the Wnt family have significant changes in exon retention after treatment with antisense morpholino (assessed by RNA-Seq and qRT-PCR, values shown are from qRT-PCR data quantifying the variable exon). The misMO oligo is a negative control that differs from the primary morpholino by 5 nucleotides in the critical binding site. The gene name is shown on the horizontal axis and the numbers represent the start position of the exon. *Significantly different from the WT, $p < 0.05$.

the level of that scaRNA but no significant change in the targeted spliceosomal RNA or in splicing of the index genes. However, when two scaRNAs were transfected together (e.g., SCARNA1 and SCARNA4), we saw a significant increase in the targeted spliceosomal RNA (i.e., U2) and an accompanying change in splice isoforms of our index genes. It was fortuitous that combining expression vectors for SCARNA1 and SCARNA4 had a significant effect on U2 levels and a concomitant effect on splicing. This is possibly because their target nucleotides are near the catalytic site so this might result in a more dramatic impact on the function of U2. In addition, SCARNA4 targets two nucleotides in U2 (uridine 39 and uridine 41) so modification of a total of three nucleotides would be affected by expression changes of these two scaRNAs. The change in isoform level reflected a change toward the normal post-natal form of the index genes. Additionally, we saw no change in the level of any other spliceosomal RNAs (e.g., U1, U4, U5, U6 and U12) after co-transfection of SCARNA1 and SCARNA4. This suggests that these effects are specific and modification of multiple nucleotides is required in order to have measurable effects on snRNA stability or function. Conversely, knockdown of scaRNAs using antisense oligos in primary cell cultures derived from normally developing heart tissue resulted in changes in the level of the targeted spliceosomal RNA when two scaRNAs were changed, but the change resulted in changes in exon retention of our index genes but not the same splice isoform pattern as in tissue with reduced scaRNAs (RV of infants with TOF). The changed levels of targeted spliceosomal RNA after simultaneous alteration of scaRNA level suggests a coordinated regulatory mechanism that may be very intricate. Further studies are needed to delineate the relative importance for spliceosomal function of individual scaRNAs, as well as synergy among scaRNAs.

4.4. scaRNA levels and splice isoforms change during normal zebrafish development

In the last decade, the zebrafish has been developed into an excellent animal model system to study cardiovascular disease and development, primarily because zebrafish embryos are not completely dependent on a functional cardiovascular system during embryonic development. In addition, the optical transparency of zebrafish embryos makes it easy to follow the course of cardiovascular development [33]. In our previous study, we successfully demonstrated for the first time that impaired rRNA modifications caused by the loss of expression of several snoRNAs lead to severe developmental defects in zebrafish [20]. Here we focus our attention on scaRNAs targeting spliceosomal RNAs. Nothing is known about the impact of these noncoding RNAs in the regulation of vertebrate development.

As a starting point, we extracted transcriptome data from the GEO and reanalyzed it to examine scaRNA expression patterns and to assess splicing transitions during the first five days of zebrafish development. There were significant changes in expression levels of multiple scaRNA during the time course examined. In addition, there were clear transitions in splicing of key genes that regulate heart development. Taken together, these observations are consistent with the possibility that scaRNA expression level and splicing transitions could be linked during zebrafish development.

4.5. Knockdown of scaRNAs alters splicing and heart development in zebrafish

Dysregulation of alternative splicing has been associated with the regulation of heart development [8,34], cardiovascular diseases [35] and several other diseases, including cancers [36]. Deficiency of the snRNP assembly factor SMN (survival of motor neuron) in a zebrafish model of spinal muscular atrophy (SMA) resulted in tissue-specific defective splicing of neurexin2 and motor axon defects [37,38]. The mutations in the tri-snRNP subunit of the pre-mRNA splicing machinery

are linked to a hereditary eye disease, retinitis pigmentosa (RP). The silencing of RP-associated splicing factor *prpf31* in zebrafish caused specific defects in vision, photoreceptor morphology and retinal gene expression [39]. However, there have been no studies targeting the RNA components of the spliceosome and their potential impact on splicing and development in vertebrates. Recently, we have reported the developmental significance of snoRNAs in zebrafish by suppressing the expression of several snoRNAs including *snord26* (U26) snoRNA [20], which was also downregulated in the myocardium of infants with TOF [17].

In this study, we have shown that specific heart defects occur after interfering with the maturation of scaRNAs by antisense morpholino oligos. We confirm that these specific defects are due to the scaRNA suppression and its effect on altered splicing of cardiac genes. These defects do not appear to be due to an off-target effect of host gene depletion, because of the detection of properly spliced *ppp1r8b* and *rrm2* mRNA transcripts in both MO and misMO injected embryos. Our previous experiments targeting snoRNAs (that target ribosomal RNAs) in zebrafish produced parallel results in that specific phenotypes were associated with the inhibition of specific snoRNAs [20]. The altered splicing of cardiac genes (e.g., *gata4*, *mbnl1*, Wnt pathway genes) might be due to the impaired 2'-O-methylation and pseudouridylation modifications on spliceosomal RNA (snRNA) caused by the inhibition of scaRNA expression. The scaRNAs targeted in our study, *scarn1* and *snord94*, direct pseudouridylation modification on U2 snRNA (U89) and 2'-O-methylation modification on U6 snRNA (C62), respectively. Although not identical, the changes in splicing we observed in 13 members of the Wnt pathway when either *scarn1* or *snord94* was targeted in zebrafish embryos were similar. Perhaps the close interaction between U2 and U6 during spliceosomal function results in a similar effect on splicing fidelity when the biochemical composition of either one is altered but this remains to be examined in future investigations.

One limitation of this study is that we have not confirmed the scaRNA inhibition that resulted in the modification of the specific target nucleotide in the spliceosomal RNA. However, based on our previous study these new findings are consistent with the concept that specific defects in the splicing of cardiac genes and heart development are derived from the impaired snRNA modifications in the zebrafish morphants. Our results indicate that dysregulated scaRNA expression, even a single scaRNA, could lead to the failure of efficient maturation and function of the target spliceosomal RNA altering the spliceosome's ability to efficiently process RNA contributing to defective organ development.

Clearly, these new findings raise additional questions. The complex interaction of multiple scaRNAs and the cumulative impact on spliceosomal fidelity needs to be more extensively evaluated. However, by analyzing the transcriptome of the RV of infants with TOF, we have identified a novel mechanism that contributes to regulatory control of the spliceosome. Our data suggest that scaRNA expression levels provide a regulatory mechanism that fine tunes spliceosome function by regulating the extent of biochemical modification of spliceosomal RNAs. During the maturation of spliceosomal RNAs, scaRNAs may regulate spliceosomal RNA stability and/or target specificity. We hypothesize that scaRNA expression level is tissue specific and if dysregulated, particularly if multiple scaRNAs are simultaneously altered, there is failure of efficient maturation or function of the snRNAs resulting in alteration in the fidelity of the spliceosome. This could in turn lead to poor transitions between mRNA splice isoform patterns during organ development. Taken in total, our observations suggest that scaRNAs modify spliceosomal RNAs in a manner essential for temporal and/or spatial integrity of spliceosome function. Thus, cardiac specific dysregulation of scaRNAs could result in reduced efficiency or fidelity of the spliceosome, leading to inaccurate splicing causing ineffective communication between the first and second heart fields and resulting in defects in the conotruncal outflow track, i.e., tetralogy of Fallot.

Supplementary data to this article can be found online at <http://dx.doi.org/10.1016/j.bbadis.2015.04.016>.

Sources of funding

Kansas City Area Life Sciences Institution, Fraternal Order of Eagles, Kansas, CMH Clinical Scholar, Katherine Barry Richards Foundation, JSPSKAKENHI Grants 2591003 (N.K.) and 24591556 (T.U.), and a grant from the Takeda Science Foundation (T.U.).

Disclosures

The authors have no conflicts of interest to declare

Transparency document

The Transparency document associated with this article can be found, in the online version.

Acknowledgements

We gratefully acknowledge Dr. Maki Yoshihama for the useful discussions during manuscript preparation and Mrs. Yukari Nakajima for her assistance with the zebrafish experiments.

References

- [1] AHA, <http://www.americanheart.org/presenter.jhtml?identifier=120122011>.
- [2] G. Andelfinger, P. Khairy, Heart to heart: challenges and perspectives for genetic research in congenital heart disease, *Expert. Rev. Cardiovasc. Ther.* 9 (2011) 655–658.
- [3] A.C. Fahed, B.D. Gelb, J.G. Seidman, C.E. Seidman, Genetics of congenital heart disease: the glass half empty, *Circ. Res.* 112 (2013) 707–720.
- [4] J. Bentham, S. Bhattacharya, Genetic mechanisms controlling cardiovascular development, *Ann. N. Y. Acad. Sci.* 1123 (2008) 10–19.
- [5] B.G. Bruneau, The developmental genetics of congenital heart disease, *Nature* 451 (2008) 943–948.
- [6] M. Buckingham, S. Meilhac, S. Zaffran, Building the mammalian heart from two sources of myocardial cells, *Nat. Rev. Genet.* 6 (2005) 826–835.
- [7] J.B. Huang, Y.L. Liu, P.W. Sun, X.D. Lv, M. Du, X.M. Fan, Molecular mechanisms of congenital heart disease, *Cardiovasc. Pathol.* 19 (2009) e183–e193.
- [8] A. Kalsotra, K. Wang, P.F. Li, T.A. Cooper, MicroRNAs coordinate an alternative splicing network during mouse postnatal heart development, *Genes Dev.* 24 (2010) 653–658.
- [9] T. Thum, D. Catalucci, J. Bauersachs, MicroRNAs: novel regulators in cardiac development and disease, *Cardiovasc. Res.* 79 (2008) 562–570.
- [10] M.W. Wessels, P.J. Willems, Genetic factors in non-syndromic congenital heart malformations, *Clin. Genet.* 78 (2010) 103–123.
- [11] N. Liu, E.N. Olson, MicroRNA regulatory networks in cardiovascular development, *Dev. Cell* 18 (2010) 510–525.
- [12] A. Kalsotra, X. Xiao, A.J. Ward, J.C. Castle, J.M. Johnson, C.B. Burge, T.A. Cooper, A postnatal switch of CELF and MBNL proteins reprograms alternative splicing in the developing heart, *Proc. Natl. Acad. Sci. U. S. A.* 105 (51) (2008) 20333–20339.
- [13] J.C. Castle, C. Zhang, J.K. Shah, A.V. Kulkarni, A. Kalsotra, T.A. Cooper, J.M. Johnson, Expression of 24,426 human alternative splicing events and predicted cis regulation in 48 tissues and cell lines, *Nat. Genet.* 40 (2008) 1416–1425.
- [14] A. Kalsotra, X. Xiao, A.J. Ward, J.C. Castle, J.M. Johnson, C.B. Burge, T.A. Cooper, A postnatal switch of CELF and MBNL proteins reprograms alternative splicing in the developing heart, *Proc. Natl. Acad. Sci. U. S. A.* 105 (2008) 20333–20338.
- [15] C.L. Will, R. Luhrmann, Spliceosome structure and function, *Cold Spring Harb. Perspect. Biol.* 3 (2011).
- [16] J. Karijolic, Y.T. Yu, Spliceosomal snRNA modifications and their function, *RNA Biol.* 7 (2010) 192–204.
- [17] J.E. O'Brien Jr., N. Kibiriyeva, X.G. Zhou, J.A. Marshall, G.K. Lofland, M. Artman, J. Chen, D.C. Bittel, Noncoding RNA expression in myocardium from infants with tetralogy of Fallot, *Circ. Cardiovasc. Genet.* 5 (2012) 279–286.
- [18] M. Charette, M.W. Gray, Pseudouridine in RNA: what, where, how, and why, *IUBMB Life* 49 (2000) 341–351.
- [19] T. Kaneko, T. Suzuki, S.T. Kapushoc, M.A. Rubio, J. Ghazvini, K. Watanabe, L. Simpson, Wobble modification differences and subcellular localization of tRNAs in *Leishmania tarentolae*: implication for tRNA sorting mechanism, *EMBO J.* 22 (2003) 657–667.
- [20] S. Higa-Nakamine, T. Suzuki, T. Uechi, A. Chakraborty, Y. Nakajima, M. Nakamura, N. Hirano, N. Kenmochi, Loss of ribosomal RNA modification causes developmental defects in zebrafish, *Nucleic Acids Res.* 40 (2012) 391–398.
- [21] D.C. Bittel, M.G. Butler, N. Kibiriyeva, J.A. Marshall, J. Chen, G.K. Lofland, J.E. O'Brien Jr., Gene expression in cardiac tissues from infants with idiopathic conotruncal defects, *BMC Med. Genet.* 4 (2011) 1.
- [22] X. Darzacq, B.E. Jady, C. Verheggen, A.M. Kiss, E. Bertrand, T. Kiss, Cajal body-specific small nuclear RNAs: a novel class of 2'-O-methylation and pseudouridylation guide RNAs, *EMBO J.* 21 (2002) 2746–2756.
- [23] G.B. Robb, K.M. Brown, J. Khurana, T.M. Rana, Specific and potent RNAi in the nucleus of human cells, *Nat. Struct. Mol. Biol.* 12 (2005) 133–137.
- [24] N. Matter, H. Konig, Targeted 'knockdown' of spliceosome function in mammalian cells, *Nucleic Acids Res.* 33 (2005) e41.
- [25] T. Uechi, Y. Nakajima, A. Nakao, H. Torihara, A. Chakraborty, K. Inoue, N. Kenmochi, Ribosomal protein gene knockdown causes developmental defects in zebrafish, *PLoS One* 1 (2006) e37.
- [26] A. Mortazavi, B.A. Williams, K. McCue, L. Schaeffer, B. Wold, Mapping and quantifying mammalian transcriptomes by RNA-Seq, *Nat. Methods* 5 (2008) 621–628.
- [27] Y. Xing, T. Yu, Y.N. Wu, M. Roy, J. Kim, C. Lee, An expectation-maximization algorithm for probabilistic reconstructions of full-length isoforms from splice graphs, *Nucleic Acids Res.* 34 (2006) 3150–3160.
- [28] A.A. Patel, J.A. Steitz, Splicing double: insights from the second spliceosome, *Nat. Rev. Mol. Cell Biol.* 4 (2003) 960–970.
- [29] J.M. Johnson, J. Castle, P. Garrett-Engele, Z. Kan, P.M. Loerch, C.D. Armour, R. Santos, E.E. Schadt, R. Stoughton, D.D. Shoemaker, Genome-wide survey of human alternative pre-mRNA splicing with exon junction microarrays, *Science* 302 (2003) 2141–2144.
- [30] G.S. Wang, T.A. Cooper, Splicing in disease: disruption of the splicing code and the decoding machinery, *Nat. Rev. Genet.* 8 (2007) 749–761.
- [31] N. Salomonis, B. Nelson, K. Vranizan, A.R. Pico, K. Hanspers, A. Kuchinsky, L. Ta, M. Mercola, B.R. Conklin, Alternative splicing in the differentiation of human embryonic stem cells into cardiac precursors, *PLoS Comput. Biol.* 5 (2009) e1000553.
- [32] F.A. Stennard, M.W. Costa, D.A. Elliott, S. Rankin, S.J. Haast, D. Lai, L.P. McDonald, K. Niederreither, P. Dolle, B.G. Bruneau, A.M. Zorn, R.P. Harvey, Cardiac T-box factor Tbx20 directly interacts with Nkx2-5, GATA4, and GATA5 in regulation of gene expression in the developing heart, *Dev. Biol.* 262 (2003) 206–224.
- [33] D. Staudt, D. Stainier, Uncovering the molecular and cellular mechanisms of heart development using the zebrafish, *Annu. Rev. Genet.* 46 (2012) 397–418.
- [34] A. Kalsotra, T.A. Cooper, Functional consequences of developmentally regulated alternative splicing, *Nat. Rev. Genet.* 12 (2011) 715–729.
- [35] E. Lara-Pezzi, A. Dopazo, M. Manzanares, Understanding cardiovascular disease: a journey through the genome (and what we found there), *Dis. Model. Mech.* 5 (2012) 434–443.
- [36] S. Oltean, D.O. Bates, Hallmarks of alternative splicing in cancer, *Oncogene* 33 (46) (2014) 5311–5318.
- [37] C. Winkler, C. Eggert, D. Gradl, G. Meister, M. Giegerich, D. Wedlich, B. Lagerbauer, U. Fischer, Reduced U snRNP assembly causes motor axon degeneration in an animal model for spinal muscular atrophy, *Genes Dev.* 19 (2005) 2320–2330.
- [38] K. See, P. Yadav, M. Giegerich, P.S. Cheong, M. Graf, H. Vyas, S.G. Lee, S. Mathavan, U. Fischer, M. Sendtner, C. Winkler, SMN deficiency alters Nrnx2 expression and splicing in zebrafish and mouse models of spinal muscular atrophy, *Hum. Mol. Genet.* 23 (2014) 1754–1770.
- [39] B. Linder, H. Dill, A. Hirmer, J. Brocher, G.P. Lee, S. Mathavan, H.J. Bolz, C. Winkler, B. Lagerbauer, U. Fischer, Systemic splicing factor deficiency causes tissue-specific defects: a zebrafish model for retinitis pigmentosa, *Hum. Mol. Genet.* 20 (2011) 368–377.